Estimation of AUV dynamics for sensor fusion

Kjell Magne Fauske
University Graduate Center
Kjeller, Norway
Email: fauske@unik.no

Fredrik Gustafsson
Department of Electrical Engineering
Linköping University
Linköping, Sweden Email: fredrik@isy.liu.se

Øyvind Hegrenæs
University Graduate Center
Kjeller, Norway
Email: hegrenas@unik.no

***Abstract*—This paper presents a method for identifying dynamic models of Autonomous Underwater Vehicles (AUV) from logged data and a physically motivated model structure. Such models are instrumental for model-based control system design, but also for integrated navigation systems. We motive our work from the perspective of developing second generation integrated navigation systems, which use a sensor fusion approach to merge external information with a dynamic model for purposes of redundancy, integrity, and for fault detection and isolation.**

Keywords: AUV, Kalman filtering, estimation.

I. Introduction

Navigation of AUVs using solely inertial sensors is not sufficient, due to the inherent drift of dead-reckoning velocities and accelerations. Support in the form of sensor fusion from Earth-fixed reference points is needed to avoid this drift. Information of this kind includes, but is not limited to, GPS fixes at the surface, acoustic baseline positioning using transponders [1], and terrain navigation [2], [3].

An aided inertial navigation system (AINS) consists basically of an error-state Kalman filter that estimates the drift parameters in the inertial sensors, using the external information as the measurement vector. Though AINS are used in various applications such as aircrafts, autonomous aerial and ground vehicles, in surface ships and underwater vehicles, these AINS usually do not take the knowledge of steering commands and dynamics of the platform into account. For navigation purposes alone, knowledge of the platform dynamics is not necessary. However, a dynamic model is of interest for achieving redundancy, and for fault detection and isolation purposes. Our goal is to investigate this, and as a crucial step, we present the results on model estimation based on experimental data. Another possible use of dynamic models is to use them as an aiding sensor. Applications include low cost AUVs with inaccurate inertial sensors, and AUVs with only compass and position aiding.

A full dynamic model of an AUV has six degrees of freedom (DOF) for position and orientation, and would require 12 states to also include all linear and angular velocities. It is well known [4], [5], that speed, steering and diving dynamics are almost decoupled for normal operation. This fact is used in control design [4], [6]. The steering dynamics is the most crucial part, since depth is measured quite accurately and speed is mostly constant in normal operation.

This paper is organized as follows. Section II gives an overview of the HUGIN 4500 AUV and its current navigation system. Section III and IV describe the kinematic and dynamic equations of motion, with an emphasis on the steering dynamics. Section V describes an identification procedure for identifying parameters of the simplified model structure. The procedure is subsequently evaluated on actual data recorded during sea trials. Potential model applications are outlined in Section VI.

Figure 1. The HUGIN 4500 autonomous underwater vehicle during deployment for sea trials.

II. System overview

A. The HUGIN 4500 AUV

The HUGIN 4500 AUV is the latest addition to the HUGIN AUV family manufactured by Kongsberg Maritime. The vehicle has a length of 6.5 meters and a nominal dry mass of approximately 1950 kg. Designed for large depths and long endurance, the vehicle can operate at depths down to 4500 meters and operate for 60-70 hours. The cruising speed of the vehicle is about 3.7 knots or 1.9 m/s. The vehicle is passively stable in roll and close to neutrally buoyant.

Typical payload sensors are sub-bottom profiler, sidescan sonar and multibeam echo sounder, all capable of running simultaneously. The vehicle can be operated in either operator supervised or autonomous mode. In the operator supervised mode an acoustic communication link is used to supervise the vehicle and to receive real-time telemetry data.

B. Control inputs

For propulsion HUGIN 4500 is fitted with a large three-bladed propeller. A cruciform tail configuration with four

identical control surfaces is used for manoeuvring (see Fig. 2).

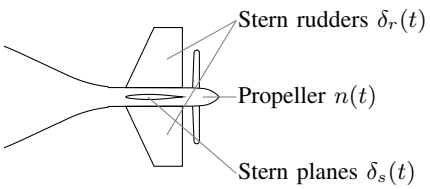

Figure 2. AUV control inputs for a cruciform tail configuration

C. Inertial navigation

The HUGIN 4500 vehicle is equipped with an inertial navigation system (INS) which calculates the position, velocity and attitude using high frequency data from an inertial measurement unit (IMU). In order to counter position error growth, an error-state Kalman filter is implemented which utilizes a wide range of aiding sensors [7]. A overview of the aided navigation system is shown in Fig. 3.

The Doppler velocity log (DVL) is of great importance for slowing the position error growth. It can measure the linear velocities of the vehicle relative to the seabed with great accuracy. For long submerged operations, position aiding is necessary. During survey missions the vehicle is usually tracked by a mother ship using ultra short baseline positioning (USBL), also known as super short baseline positioning (SSBL). Position updates are then transmitted regularly to the vehicle using an acoustic communication link (see Fig. 4).

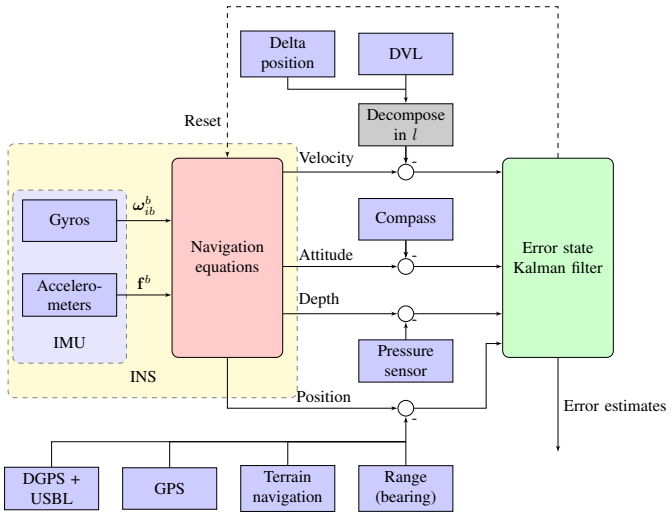

Figure 3. Aided inertial navigation system

III. Underwater vehicle kinematics

Six independent coordinates are required to completely describe the position and orientation of an underwater vehicle. For marine vehicles it is common to use the SNAME [8] notation summarized in Table I.

The coordinates are grouped into two vectors, where

$$\boldsymbol{\eta} = \begin{bmatrix} x & y & z & \phi & \theta & \psi \end{bmatrix}^{\mathrm{T}} \tag{1}$$

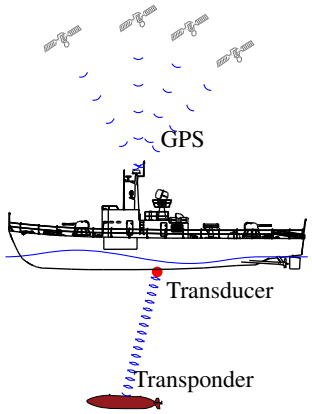

Figure 4. GPS+ultra short baseline (USBL) tracking of AUV

Table I
THE SNAME NOTATION FOR MARINE VESSELS

Motion components	Forces and moments	Linear and angular velocities	Position and Euler angles
surge (x-direction)	X	u	x
sway (y-direction)	Y	v	y
heave (z-direction)	Z	w	z
roll (rotation about x)	K	p	ϕ
pitch (rotation about y)	M	q	θ
yaw (rotation about z)	N	r	ψ

denotes the position and orientation, and

$$\boldsymbol{\nu} = \begin{bmatrix} u & v & w & p & q & r \end{bmatrix}^{\mathrm{T}} \tag{2}$$

denotes linear and angular velocities. The position coordinates

$$\boldsymbol{p}^e = \begin{bmatrix} x & y & z \end{bmatrix}^{\mathrm{T}} \tag{3}$$

are decomposed in an Earth-centered and Earth-fixed frame (ECEF). However, for local navigation it is convenient to use a local North East Down (NED) coordinate frame instead. Linear and angular velocities are decomposed in the body fixed frame.

The 6DOF kinematic equations are written as

$$\dot{\boldsymbol{\eta}} = \boldsymbol{J}(\boldsymbol{\eta})\boldsymbol{\nu}, \tag{4}$$

where $\boldsymbol{J}(\boldsymbol{\eta})$ is a nonlinear transformation matrix.

IV. Underwater vehicle dynamics

The nonlinear dynamic equations of motion can be expressed in a compact form as [9]:

$$\dot{\boldsymbol{\eta}} = \boldsymbol{J}(\boldsymbol{\eta})\boldsymbol{\nu} \tag{5a}$$

$$\boldsymbol{M}\dot{\boldsymbol{\nu}} + \boldsymbol{C}(\boldsymbol{\nu})\boldsymbol{\nu} + \boldsymbol{D}(\boldsymbol{\nu})\boldsymbol{\nu} + \boldsymbol{g}(\boldsymbol{\eta}) = \boldsymbol{\tau} + \boldsymbol{w}, \tag{5b}$$

where $\boldsymbol{M}$ is the inertia matrix of the vehicle including added mass, $\boldsymbol{C}(\boldsymbol{\nu}) = \boldsymbol{C}_{RB}(\boldsymbol{\nu}) + \boldsymbol{C}_A(\boldsymbol{\nu})$ is the centrifugal and coriolis matrix, $\boldsymbol{D}(\boldsymbol{\nu})$ is the hydrodynamic damping matrix, $\boldsymbol{g}(\boldsymbol{\nu})$ is the vector of gravity and buoyant forces, $\boldsymbol{\tau}$ is the control input vector of forces and moments, and $\boldsymbol{w}$ is a vector of environmental disturbances.

The vehicle dynamics are affected by currents. Taking this into account, a more accurate model can be given as

$$\boldsymbol{M}\dot{\boldsymbol{\nu}} + \boldsymbol{C}_{RB}(\boldsymbol{\nu})\boldsymbol{\nu} + \boldsymbol{C}_A(\boldsymbol{\nu}_r)\boldsymbol{\nu}_r + \boldsymbol{D}(\boldsymbol{\nu}_r)\boldsymbol{\nu}_r + \boldsymbol{g}(\boldsymbol{\eta}) = \boldsymbol{\tau} + \boldsymbol{w}, \quad (6)$$

where

$$\boldsymbol{\nu}_r = \boldsymbol{\nu} - \boldsymbol{\nu}_c \quad (7)$$

is the velocity of the vehicle relative to the surrounding fluid. In open waters the current, $\boldsymbol{\nu}_c$, is often assumed to be irrotational and can be written as

$$\boldsymbol{\nu}_c = \begin{bmatrix} u_c & v_c & w_c & \mathbf{0}_{1\times 3} \end{bmatrix}. \quad (8)$$

In this article the current velocity is assumed to be very small, and (5) will be used. Underwater currents will however nearly always be present and need to be handled. A common method is to model the current as a slowly varying bias.

Equation (5) is not practical for controller or observer design. For slender and symmetric vehicles it is possible to separate the system into three noninteracting (or lightly interacting) systems [6], [9], [10]. The three subsystems and their state variables are:

- Speed: $u(t)$
- Steering: $v(t), r(t), \psi(t)$
- Diving: $w(t), q(t), \theta(t), z(t)$

The subsystems with states and control inputs for a cruciform tail configuration, are summarized in Table II. See also Fig. 2.

Table II
DECOUPLED SUBSYSTEMS OF AN UNDERWATER VEHICLE

Subsystem	State variables	Control inputs
Speed	$u(t)$	$n(t)$
Steering	$v(t), r(t), \psi(t)$	$\delta_r(t)$
Diving	$w(t), q(t), \theta(t), z(t)$	$\delta_s(t)$

In the following, simplified models of the speed, steering and diving subsystems will be given, based on [5], [6]. The SNAME notation in Table I will be used for denoting forces and moments.

For more detailed models of the HUGIN 4500 AUV see [11]. More general information about marine vehicle dynamics can be found in for instance [5], [9].

A. Speed subsystem

Neglecting interactions from other parts of the system, the surge subsystem can be modeled as

$$(m - X_{\dot{u}})\dot{u} - X_u u - X_{|u|u}|u|u = \tau_1(n) + T_{\text{loss}}, \quad (9)$$

where m and $X_{\dot{u}}$ denote vehicle mass and added mass respectively, X_u is linear damping, $X_{|u|u}$ is quadratic damping, and T_{loss} contains coupling terms and environmental disturbances. For low speed applications $X_{|u|u} \approx 0$. The propeller dynamics can be modeled as

$$\tau_1 = T_{|n|n}|n|n + T_{|n|u}|n|u \quad (10)$$

where $T_{|n|n}$ and $T_{|n|u}$ are propeller coefficients an n is the propeller revolution.

The HUGIN AUV speed controller usually tries to maintain a constant propeller revolution rate instead of trying to maintain a constant surge speed u_0. This is to optimize the battery operation. As a consequence the surge speed u will drop somewhat during maneuvers due to some coupling between the surge and the steering subsystem.

B. Steering subsystem

Under the assumption of nearly constant speed $u \approx u_0$, the vehicle dynamics in sway and yaw can be simplified to:

$$m\dot{v} + mu_0 r = Y \quad (11)$$
$$I_z\dot{r} = N, \quad (12)$$

where

$$Y = Y_{\dot{v}}\dot{v} + Y_{\dot{r}}\dot{r} + Y_v v + Y_r r + Y_\delta \delta_r \quad (13)$$
$$N = N_{\dot{v}}\dot{v} + N_{\dot{r}}\dot{r} + N_v v + N_r r + N_\delta \delta_r. \quad (14)$$

For small roll and pitch angles we can assume that

$$\dot{\psi} \approx r. \quad (15)$$

The steering subsystem can then be rearranged as

$$\begin{bmatrix} m - Y_{\dot{v}} & -Y_{\dot{r}} & 0 \\ -N_{\dot{v}} & I_z - N_{\dot{r}} & 0 \\ 0 & 0 & 1 \end{bmatrix} \begin{bmatrix} \dot{v} \\ \dot{r} \\ \dot{\psi} \end{bmatrix} + \begin{bmatrix} -Y_v & -Y_r + mu_0 & 0 \\ -N_v & -N_r & 0 \\ 0 & -1 & 0 \end{bmatrix} \begin{bmatrix} v \\ r \\ \psi \end{bmatrix} = \begin{bmatrix} Y_\delta \\ N_\delta \\ 0 \end{bmatrix} \delta_r. \quad (16)$$

Writing the above equation in state space form yields

$$\begin{bmatrix} \dot{v} \\ \dot{r} \\ \dot{\psi} \end{bmatrix} = \begin{bmatrix} a_{11} & a_{12} & 0 \\ a_{21} & a_{22} & 0 \\ 0 & 1 & 0 \end{bmatrix} \begin{bmatrix} v \\ r \\ \psi \end{bmatrix} + \begin{bmatrix} b_1 \\ b_2 \\ 0 \end{bmatrix} \delta_r. \quad (17)$$

To calculate the horizontal position, kinematic differential equations are needed

$$\dot{x} = u\sin\psi + v\cos\psi \quad (18)$$
$$\dot{y} = u\cos\psi - v\sin\psi. \quad (19)$$

C. Depth dynamics

A neutrally buoyant vehicle dives using its stern planes and forward motion. The vehicle depth dynamics can be simplified to

$$m(\dot{w} - u_0 q) = Z \quad (20)$$
$$I_y\dot{q} = M, \quad (21)$$

where Z and M are forces and moments due to added mass, damping and stern plane deflection. Expanding the terms gives the model

$$\begin{bmatrix} m - Z_{\dot{w}} & -Z_{\dot{q}} & 0 & 0 \\ -M_{\dot{w}} & I_y - M_{\dot{q}} & 0 & 0 \\ 0 & 0 & 1 & 0 \\ 0 & 0 & 0 & 1 \end{bmatrix} \begin{bmatrix} \dot{w} \\ \dot{q} \\ \dot{\theta} \\ \dot{z} \end{bmatrix} + \begin{bmatrix} -Z_w & mu_0 - Z_q & 0 & 0 \\ -M_w & -M_q & \overline{BG}_z W & 0 \\ 0 & -1 & 0 & 0 \\ -1 & 0 & u_0 & 0 \end{bmatrix} \begin{bmatrix} w \\ q \\ \theta \\ z \end{bmatrix} = \begin{bmatrix} Z_\delta \\ M_\delta \\ 0 \\ 0 \end{bmatrix} \delta_s, \quad (22)$$

where $W = mg$ and $\overline{BG}_z$ is a moment caused by a difference between the center of gravity and center of buoyancy.

Writing the above equation in state space form yields

$$\begin{bmatrix} \dot{w} \\ \dot{q} \\ \dot{\theta} \\ \dot{z} \end{bmatrix} = \begin{bmatrix} c_{11} & c_{12} & c_{13} & 0 \\ c_{21} & c_{22} & c_{23} & 0 \\ 0 & 1 & 0 & 0 \\ 1 & 0 & -u_0 & 0 \end{bmatrix} \begin{bmatrix} w \\ q \\ \theta \\ z \end{bmatrix} + \begin{bmatrix} d_1 \\ d_2 \\ 0 \\ 0 \end{bmatrix} \delta_s. \quad (23)$$

The heave speed, w, is usually low, so the above model can be simplified to

$$\begin{bmatrix} \dot{q} \\ \dot{\theta} \\ \dot{z} \end{bmatrix} = \begin{bmatrix} c_{22} & c_{23} & 0 \\ 1 & 0 & 0 \\ 0 & -u_0 & 0 \end{bmatrix} \begin{bmatrix} q \\ \theta \\ z \end{bmatrix} + \begin{bmatrix} d_2 \\ 0 \\ 0 \end{bmatrix} \delta_s. \quad (24)$$

D. Model discussion

The steering model (17) and diving model (23) are in a convenient linear form. However, finding the lumped coefficients a_{ij}, b_i, c_{ij}, d_i is a nontrivial task. The coefficients can be calculated if the physical vehicle parameters are known. Another approach is to estimate the coefficients directly from (17) or (23) using measurements of the states v, r, w, q, θ and the control inputs δ_r and δ_s. This approach will be investigated in Section V for the steering dynamics.

The downside of estimating the parameter vector (25) directly, is that the identified parameters do not have a clear physical interpretation. Some of the parameters will in fact be slowly time varying. This is mostly because the mass m of the vehicle decreases slowly as the battery is depleted. The parameters are also dependent on the cruising speed u_0. A change in cruising speed will alter the model. For practical implementations a solution may be to utilize online parameter identification techniques, model switching, or express the uncertainty as process noise.

The AUV dynamics are inherently nonlinear. However, the linear models capture the most important dynamics and are accurate enough for applications like decoupled autopilot design and model-based fault detection.

V. Identification procedure

Of the three almost decoupled subsystems mentioned in Section IV, the steering dynamics is the most challenging one. Depth is measured quite accurately, and the motor runs at constant rpm most of the time, giving poor excitation of the speed dynamics. We will here describe how state-of-the art algorithms are used to find a dynamic model that enables accurate simulation of the steering dynamics. Simulation is in fact much more than what is required by sensor fusion algorithms for integrated navigation, fault diagnosis and control, where only the predictive ability of the model is important. The one-step or short-time prediction of a model is usually much more accurate than a batch simulation.

In summary, the system identification task is to estimate the parameters

$$\boldsymbol{\theta} = \begin{bmatrix} a_{11} & a_{12} & a_{21} & a_{22} & b_1 & b_2 \end{bmatrix}^{\mathrm{T}} \quad (25)$$

in the continuous-time physical model structure (17), given observations of $(v(t), r(t), \delta_r(t))$ and the non-uniform sampling times t_k, $k = 1, 2, \ldots, N$.

For the parameter identification, data collected during a sea-trial mission with the HUGIN 4500 vehicle were used. Prior to applying the identification procedure, the measurements were outlier filtered and smoothed using the navigation post-processing tool NavLab [12]. This was done in order to enhance the accuracy.

The classical identification area concerns estimation of discrete time black box models from uniform sampled data [13]. We are here facing a grey-box identification problem, where there are still no standardized approaches [14], [15]. Our approach is based on the non-linear least squares (NLS) criteria

$$\hat{\boldsymbol{\theta}} = \arg\min_{\boldsymbol{\theta}} \sum_{k=1}^{N} \left(\mathbf{y}(t_k) - \hat{\mathbf{y}}(t_k; \boldsymbol{\theta}) \right)^2, \quad (26)$$

where $\mathbf{y}(t_k) = [v(t_k)\ r(t_k)]^{\mathrm{T}}$ is the measurement vector, and $\mathbf{y}(t_k; \boldsymbol{\theta})$ is the simulation of the dynamic model (17) using the parameter vector $\boldsymbol{\theta}$.

The complete approach is as follows:

1) In order to get good initial values to the NLS optimization, a discrete time transfer function is first estimated. The single input multiple output (SIMO) model structure follows from (17) as

$$\begin{bmatrix} v(kT) \\ r(kT) \end{bmatrix} = G(z)\delta_r(kT). \quad (27)$$

This is identified using the following steps (see [13] for definitions and details):

   a) Resample the data regularly at a sampling frequency of 1Hz.
   b) Estimate a high order finite impulse response (FIR) model, where $G(z)$ has only zeros, no poles. This is done by the least squares method.
   c) Simulate noise-free measurements using the FIR model and true input.

d) Estimate $G(z)$ as an autoregressive with exogenous input ARX(2,2,1) model using the least squares method.

The ARX model could be estimated directly in step 2 above. The point with the second and third step is that a so called output error model is obtained, which is much better suited for simulation than an ARX model. The resulting transfer function is

$$\begin{aligned} Y_1(z) &= \frac{1.48 \cdot z + 1.02}{z^2 + 3.63 \cdot z + 0.338} U(z) \\ Y_2(z) &= \frac{-35.5 \cdot z - 11.2}{z^2 + 3.63 \cdot z + 0.338} U(z). \end{aligned} \tag{28}$$

2) The discrete time transfer function is converted to a continuous time state space model with the structure (17) using the following steps:
   a) Convert discrete time transfer function to discrete time state space model.
   b) Apply inverse sampling to get a continuous time model.
   c) Make a change of state variables to $\boldsymbol{x} := \boldsymbol{C}^{-1}\boldsymbol{x}$ so that the $\boldsymbol{C}$ matrix becomes the identity matrix in the new coordinates.

   The resulting model is already on the form (17):

$$\begin{aligned} \dot{\boldsymbol{x}}(t) &= \begin{bmatrix} 1.555 & 0.187 \\ -44.925 & -5.183 \end{bmatrix} \boldsymbol{x}(t) + \begin{bmatrix} 1.476 \\ -35.475 \end{bmatrix} u(t) \\ \boldsymbol{y}(t) &= \begin{bmatrix} 1.000 & 0.000 \\ 0.000 & 1.000 \end{bmatrix} \boldsymbol{x}(t). \end{aligned} \tag{29}$$

3) **NLS optimization.** The Gauss-Newton algorithm is applied to (26), using a continuous time ordinary differential equation (ODE) solver to produce the simulated $\hat{\mathbf{y}}(t_k)$ at non-uniformly sampled data. The ODE solver handles non-linear continuous time ODEs, though the model here is linear in the states.

Table III
ITERATIONS OF THE GAUSS-NEWTON ALGORITHM APPLIED TO (26)

Iteration	Cost	Gradient norm
0	$5.602 \cdot 10^2$	-
1	$5.531 \cdot 10^2$	$4.890 \cdot 10^3$
2	$5.525 \cdot 10^2$	$3.965 \cdot 10^3$

The iterations of the Gauss-Newton algorithm are shown in Table III. In this case, the NLS cost (26) decreased only marginally, and there are only minor changes in the parameters:

$$\begin{aligned} \dot{\boldsymbol{x}}(t) &= \begin{bmatrix} 1.529 & 0.190 \\ -44.970 & -5.355 \end{bmatrix} \boldsymbol{x}(t) + \begin{bmatrix} 1.490 \\ -35.586 \end{bmatrix} u(t) \\ \boldsymbol{y}(t) &= \begin{bmatrix} 1.0 & 0.0 \\ 0.0 & 1.0 \end{bmatrix} \boldsymbol{x}(t). \end{aligned} \tag{30}$$

4) **Validation by simulation.**
Fig. 5 shows the simulation of the identified discrete time model, final continuous time model, and measurements. Both models have a good fit, but have some overshoot during turns where the rudders are saturated. This is probably due to the fact that surge speed u decreases slightly during maneuvers. The assumption of constant surge speed u_0 is therefore violated.

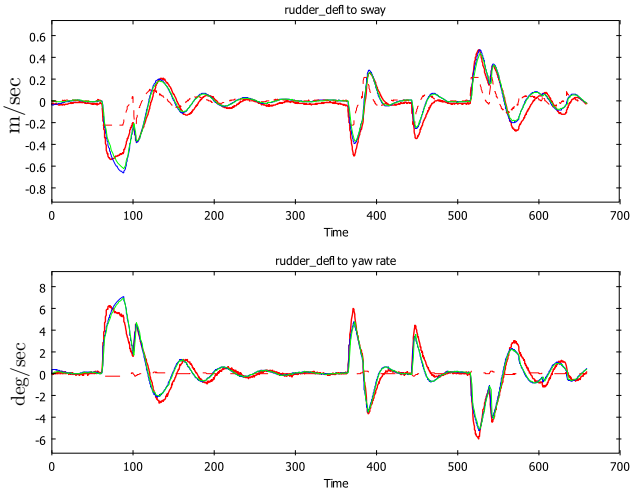

Figure 5. Simulation of identified discrete time model, final continuous time model and measurements. Heavy lines are measured values. Time is given in seconds. Rudder deflection is shown as a dashed line (in radians).

5) **Cross validation.** A standard step in system identification to prevent over fitting observed data, is to validate the model on a new data set not used for estimation. An example with excellent performance is shown in Fig. 6. In this case the identified models were simulated using rudder inputs recorded on a different part of the sea-trial mission.

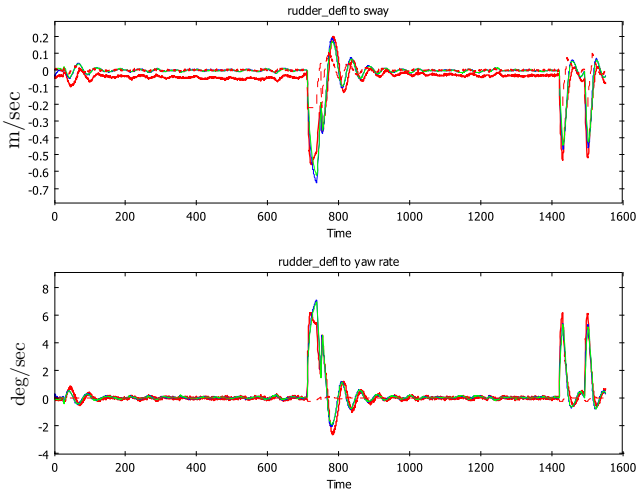

Figure 6. Same as Fig. 5, but using cross validation on new data.

VI. APPLICATIONS

Approximate models of underwater vehicle dynamics have been successfully applied to controller design [4], [6] and

for model-based fault detection [16]–[20]. Many of the fault detection schemes are designed for detecting actuator faults, with the goal of achieving fault tolerant and robust control. For vehicles with redundant actuation, the control reallocation problem is a challenging subproblem. [20]

Underwater vehicles like HUGIN have little actuator redundancy. In the event of an actuator failure, the vehicle has to abort the mission. Extensive sea trials have shown that for survey missions with HUGIN, sensor faults are a larger problem than actuator faults.

From a navigation point of view, a dynamic model can be used as an aiding sensor. Of special interest is the estimation of linear velocities, which usually are measured using a DVL. Due to environmental uncertainties, a model will not be as accurate as a DVL. However, the estimated velocities can be used to bound the velocity error. For vehicles equipped with a DVL, dynamic models can be used to do residual testing.

Outliers are a problem for sensors based on acoustics, like for instance baseline positioning systems. Variations in seawater density, temperature and salinity result in raybending and multipath propagation. This, together with environmental disturbances, often results in spurious measurements. For a mother ship tracking an underwater vehicle this can be seen as a maneuvering target tracking problem [22]. A physically motivated target model will improve the tracking performance [23] and help to detect outliers. Some initial results on USBL outlier filtering have been reported in [21].

VII. Conclusion

In this paper, a procedure for identifying dynamic models of underwater vehicles from logged data and a physically motivated model structure was developed. The procedure was applied to the simplified steering dynamics with excellent results. The work was motivated by the perspective of using the models for sensor fusion and for fault detection and isolation. This will be the subject of future papers.

Acknowledgment

The authors are grateful to Kongsberg Maritime and the Norwegian Defence Research Establishment (FFI) for providing post-processing software and data from HUGIN 4500 sea trials.

References

[1] M. Mandt, K. Gade, and B. Jalving, "Integrating DGPS-USBL position measurements with inertial navigation in the HUGIN 3000 AUV," in *Proceedings of the 8th Saint Petersburg International Conference on Integrated Navigation Systems*, Saint Petersburg, Russia, 2001.

[2] R. Karlsson and F. Gustafsson, "Bayesian surface and underwater navigation," *IEEE Transactions on Signal Processing*, vol. 54, no. 11, pp. 4204–4213, Nov. 2006.

[3] K. B. Ånonsen and O. Hallingstad, "Terrain aided underwater navigation using point mass and particle filters," in *Proc. IEEE/ION Position, Location, And Navigation Symposium*, Apr. 25–27, 2006, pp. 1027–1035.

[4] A. Healey and D. Lienard, "Multivariable sliding mode control for autonomous diving and steering of unmanned underwater vehicles," *IEEE Journal of Oceanic Engineering*, vol. 18, no. 3, pp. 327–339, Jul. 1993.

[5] T. I. Fossen, *Guidance and Control of Ocean Vehicles*. New York: Wiley, 1994.

[6] B. Jalving, "The NDRE-AUV flight control system," *IEEE Journal of Oceanic Engineering*, vol. 19, no. 4, pp. 497–501, Oct. 1994.

[7] B. Jalving, K. Gade, O. K. Hagen, and K. Vestgard, "A toolbox of aiding techniques for the HUGIN AUV integrated inertial navigation system," *Modeling, Identification and Control*, vol. 25, no. 3, pp. 173–190, Jul. 2004.

[8] SNAME, "The society of naval architects and marine engineers. nomenclature for treating the motion of a submerged body through a fluid," *Technical and Research Bulletin*, vol. 1–5, 1950.

[9] T. I. Fossen, *Marine Control Systems. Guidance, Navigation, and Control of Ships, Righs and Underwater Vehicles*. Trondheim, Norway: Marine Cybernetics, 2002.

[10] L. Ni, "Fault-tolerant control of unmanned underwater vehicles," Ph.D. dissertation, Virginia Polytechnic Institute and State University, Department of Mechanical Engineering, 2001.

[11] Ø. Hegrenæs, O. Hallingstad, and B. Jalving, "Comparison of mathematical models for the HUGIN 4500 AUV based on experimental data," in *International Symposium on Underwater Technology (UT'07)*, Tokyo, Apr. 2007, (To appear).

[12] K. Gade, "Navlab, a generic simulation and post-processing tool for navigation," *European Journal of Navigation*, vol. 2, no. 4, pp. 21–59, Nov. 2004.

[13] L. Ljung, *System Identification – Theory For the User*, 2nd ed. Upper Saddle River, N.J.: Prentice Hall, 1999.

[14] S. F. Graebe and T. Bohlin, "Identification of nonlinear stochastic grey box models: theory, implementation, and experiences," in *Selected Papers from the 4th IFAC Symposium on Adaptive Systems in Control and Signal Processing 1992.*, ser. IFAC Symposia Series, no. 8, Grenoble, France, 1993, pp. 47–52.

[15] T. Bohlin, *Practical Grey-box Process Identification: Theory and Applications*. London: Springer-Verlag, 2006.

[16] Y. K. Alekseev, V. V. Kostenko, and A. Y. Shumsky, "Use of identification and fault diagnostic methods for underwater robotics," in *Proc. OCEANS '94*, vol. 2, Brest, Sep. 1994.

[17] A. Alessandri, M. Caccia, and G. Veruggio, "A model-based approach to fault diagnosis in unmanned underwater vehicles," in *Proc. OCEANS '98*, vol. 2, Nice, Sep./Oct. 1998, pp. 825–829.

[18] ——, "Fault detection of actuator faults in unmanned underwater vehicles," *Control Engineering Practice*, vol. 7, no. 3, pp. 357–68, Mar. 1999.

[19] L. Ni and C. Fuller, "Control reconfiguration based on hierarchical fault detection and identification for unmanned underwater vehicles," *Journal of Vibration and Control*, vol. 9, no. 7, pp. 735–48, Jul. 2003.

[20] G. Antonelli, *Fault Diagnosis and Fault Tolerance for Mechatronic Systems: Recent Advances*, ser. Springer Tracts in Advanced Robotics. Springer Berlin / Heidelberg, 2003, ch. A Survey of Fault Detection/Tolerance Strategies for AUVs and ROVs, pp. 109–127.

[21] K. M. Fauske and O. Halingstad, "A comparison of outlier detection algortihms for hydro-acoustic positioning," in *Proc. MTS/IEEE OCEANS'06*, Boston, MA, Sep. 2006.

[22] Y. Bar-Shalom, X. R. Li, and T. Kirubarajan, *Estimation With Applications to Tracking and Navigation*. John Wiley & Sons, Inc., 2001.

[23] X. Rong Li and V. Jilkov, "Survey of maneuvering target tracking. part i. dynamic models," *IEEE Transactions on Aerospace and Electronic Systems*, vol. 39, no. 4, pp. 1333–1364, Oct. 2003.